Layered ammines

DOI: 10.1002/anie.201207082

The Layered Structure of $[Na(NH_3)_4][Indenide]$ Containing a Square-Planar $Na(NH_3)_4^+$ Cation**

Reent Michel, Tobias Nack, Roman Neufeld, Johannes M. Dieterich, Ricardo A. Mata, and Dietmar Stalke**

Layered structures and intercalation compounds play an outstanding role in materials science. Most prominent are graphite intercalation compounds owing to their use in energy storage by lithium-ion batteries (LiC_6),[1] synthesis (KC_8),[2] and their features concerning supraconductivity (CaC_6).[3] Self-assemblies of charged supramolecular sandwich structures formed by polycyclic carbanions and lithium cations are expected to be structural motifs of charged anode materials in prospective rechargeable batteries fabricated from carbon allotropes.[4] In inorganic chemistry (strongly intersecting with materials science), layered structures and intercalation are prominent in lithium transition-metal oxides[5] as cathode material in lithium-ion batteries and M_xFeS and M_xFeSe as potent high-temperature superconducting materials.[6] To date, in general, the layer host material is strongly bonded within the plane and exhibits weak interactions between the layers. Graphite or transition-metal oxide layer sheets are reduced by the desired metal or alloy to form anionic layers, and the cations, normally stripped of the solvent molecules, slip between these charged layers.

While extended layered structures are known from inorganic metal oxides and annulated carbon rings, this structural motif is currently unprecedented in organometallic chemistry from small molecules. To establish a similar scaffold in this array, self-assembly is required. The single building blocks must be charged, flat in shape to form an infinite layer, and have to provide intermolecular attraction to form the material. A small flat and charged building block is the indenyl anion (Ind^-). It can easily be obtained by deprotonation of indene and provides a C_5- and/or C_6-carbanionic perimeter for π-coordination. It is a widespread starting material in organometallic synthesis to generate sandwich or half-sandwich d-block organometallic compounds, which are applied in a vast number of catalytic reactions.[7] Compared to cyclopentadienide (Cp), the additional six-membered ring dilutes the charge distribution and leaves it less attractive to metal ions. To create the cationic building block, the tendency of hard metal ions to form solvent-separated ion pairs (SSIPs) can be employed. The interaction of the cation with the π system can be disfavored by supplying enough electron density by coordinating donor bases. In the past, ammonia has proven to be very effective in solvent separation of CpLi to form $[Li(NH_3)_4][Cp]\cdot NH_3$.[8] The high dipole moment ($\mu = 1.47$ D)[9] and the low steric requirements lead to a high electron-density shift to the metal ion, improving the solubility by coordination. To create a cationic building block, sodium is the metal of choice. In contrast to Li, K, Cu, and Ag, which tend to form distorted tetrahedral complexes of $[M(TMEDA)_2]$ (TMEDA = *N*′,*N*′,*N*,*N*-tetramethylethylenediamine) or interact with the chemical environment, it adopts a square-planar coordination pattern like $[Ni(TMEDA)_2]$ (Cambridge Structural Database (CSD) entries[10] for $[M(TMEDA_2)]$: Na 10, Ni 1, K 2, Li 110, Cu 6, Ag 1; for details, see the Supporting Information). We expected that the exchange of the bulky chelating donor base in the established pattern by ammonia might yield a flat cationic building block suitable in size and geometry for Ind^-.

A straightforward approach to obtain both Ind^- and $Na(NH_3)_4^+$ is by saturating a solution of indene and $[Na\{N(SiMe_3\}_2]$ in Et_2O at −15 °C with gaseous ammonia. At −16 °C $[Na(NH_3)_4][Ind]$ (**1**) crystallizes in the monoclinic space group $P2_1$ as a solvent-separated ion pair (Figure 1).

Indeed, $[Na(NH_3)_4][Ind]$ forms a rippled layer structure with alternating cationic layers of $Na(NH_3)_4^+$ and anionic layers of Ind^-. The average plane of the NH_3-coordinated cation is tilted by 10.1°(2) with respect to the indenyl planes. The interlayer distance between the aromatic carbanions of $d = 6.04$ Å is much smaller than twice the distance in graphite

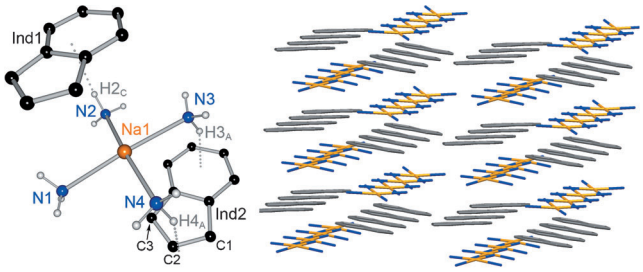

Figure 1. Crystal structure of $[Na(NH_3)_4][Ind]$ (**1**). Left: Ind2 is generated by symmetry. C—H hydrogen atoms were omitted for clarity. Ind···H interactions are drawn perpendicular to the indenyl plane. Bond lengths [Å] and angles [°]: Na1–N1 2.489(2), Na1–N2 2.458(2), Na1–N3 2.500(2), Na1–N4 2.451(2); N1-Na1-N2 92.41(6), N1-Na1-N3 174.67(6), N1-Na1-N4 90.75(6), N2-Na1-N3 87.38(5), N2-Na1-N4 175.48(6), N3-Na1-N4 89.18(5), Ind···H: $H2_C$ 2.52(2), $H3_A$ 2.47(2), $H4_A$ 2.54(2). Right: packing plot of **1**.

[*] R. Michel, T. Nack, R. Neufeld, Prof. Dr. D. Stalke
Institut für Anorganische Chemie der Universität Göttingen
Tammannstrasse 4, 37077 Göttingen (Germany)
E-mail: dstalke@chemie.uni-goettingen.de
Dr. J. M. Dieterich, Prof. Dr. R. A. Mata
Institut für Physikalische Chemie der Universität Göttingen
Tammannstrasse 6, 37077 Göttingen (Germany)

[**] We kindly acknowledge funding from the DFG Priority Programme 1178 and the DNRF funded Centre of Materials Crystallography.
Supporting information for this article is available on the WWW under http://dx.doi.org/10.1002/anie.201207082.

(6.708 Å).[1] No strong interactions are observed between the sodium ion and the indenyl rings, with the shortest distances found at 2.957(2) Å and 3.084(2) Å, respectively. The largest C_5–Na distance filed in the CSD for aromatic contact ion pairs is 2.763 Å and the average distance is 2.452 Å (for details, see the Supporting Information).[10]

The square-planar $Na(NH_3)_4^+$ cation is an unprecedented coordination motif in alkali-metal coordination. The valence shell of Na^+ is roughly spherical and has no tendency to form square-planar complexes. Six-fold coordination is by far the most frequent pattern, mirrored by 2210 hits in the CSD compared to 795 hits for fourfold coordination (for more details, see the Supporting Information).[10] The latter entries also include many sixfold coordinated structures that are not correctly assigned by missing additional contacts.

To elucidate the influence of the indenyl anions, the ammonia donors and metal hardness, the derivatives containing Li and K were prepared analogously. $[Li(NH_3)_4][Ind]$ (**2**) was synthesized by adding $[Li\{N(SiMe_3\}_2]$ and indene to a mixture of THF and Et_2O, saturated with gaseous ammonia at −15 °C, and stored for crystallization at −16 °C. Compound **2** crystallizes in the orthorhombic space group $P2_12_12_1$ (Figure 2). As in **1**, the asymmetric unit consists of a SSIP of an indenyl anion and a lithium cation *N*-coordinated by four ammonia molecules (Figure 2).

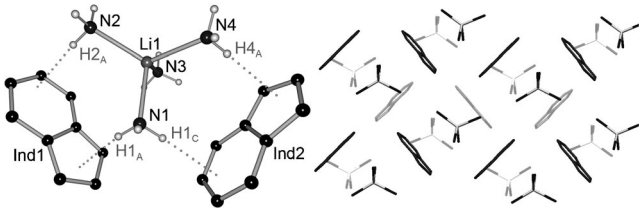

Figure 2. Crystal structure of $[Li(NH_3)_4][Ind]$ (**1**). Left: Ind2 is generated by symmetry. C–H hydrogen atoms were omitted for clarity. Ind···H interactions are drawn perpendicular to the indenyl plane. Bond lengths [Å] and angles [°]: Li1–N1 2.029(2), Li1–N2 2.071(2), Li1–N3 2.063(2), Li1–N4 2.070(2); N1-Li1-N2 111.02(7), N1-Li1-N3 104.90(7), N1-Li1-N4 104.06(7), N2-Li1-N3 107.36(7), N2-Li1-N4 121.95(8), N3-Li1-N4 107.36(7), Ind···H: $H1_A$ 2.47(2), $H2_A$ 2.72(2), $H1_C$ 2.55(2), $H4_A$ 2.49(2). Right: Packing plot of **1**, neighboring zigzag layer in the back is depicted transparently.

In contrast to $Na(NH_3)_4^+$, the lithium ion is tetrahedrally coordinated by the four ammonia molecules owing to its higher charge concentration and therefore higher attraction to the lone pairs of NH_3. The Li–N distances are on average 2.058 Å long, in contrast to 2.475 Å for Na–N in **1**, reflecting the difference in radius. The indenyl anions are arranged in a zigzag fashion relative to the $Li(NH_3)_4$ cations, with the indenyl anions facing N1/N2 and N1/N4 in alteration.

The switch of sodium to potassium leads to a different but already known structural motif of a coordination polymer such as in [(TMEDA)K(Ind)] consisting of contact ion pairs (CIPs).[11] $[(H_3N)_2K(Ind)]_\infty$ (**3**) was synthesized by saturating a mixture of indene and $[K\{NSiMe_3\}_2]$ in Et_2O with gaseous ammonia at −15 °C and crystallized at −45 °C in the orthorhombic space group *Fddd* with one fully occupied Ind^- and two half occupied $K(NH_3)_2^+$ units. In contrast to **1** and **2**, the potassium ions coordinate the indenyl anions at the five-membered rings, forming a helical coordination polymer (Figure 3).

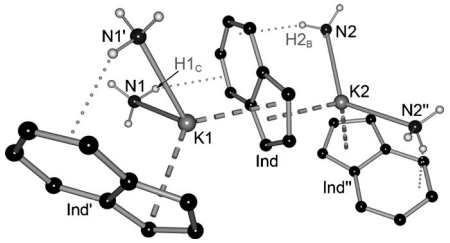

Figure 3. Crystal structure of $[(H_3N)_2K(Ind)]_\infty$ (**3**). C–H hydrogen atoms were omitted for clarity. (′) and (″) indicate two different symmetry operations. Ind···H and Ind-K interactions are drawn perpendicular to the indenyl plane. Bond lengths [Å] and angles [°]: K1–N1 2.836(2), K2–N2 2.796(2); N1-K1-N1′ 88.87(8), N2-K2-N2″ 127.05(6), Ind···$H1_C$ 2.59(2), Ind···$H2_B$ 2.74(2), Ind···K1 2.8811(6), Ind···K2 2.8712(6).

The η^5-coordination of K^+ to Ind^- meets the Pearson HSAB concept, a soft cation (K^+) interacting stronger with a soft anion (Ind^-) than a hard cation (Li^+, Na^+). Obviously the coordination strength of NH_3 is not sufficient to generate a SSIP. Instead it simply fills the coordination sphere of K^+ in a CIP. The N-K-N angles are related to the different arrangement of the indenyl anions along the Ind-K-Ind backbone. For the smaller N1-K1-N1′ angle of 88.87(8)°, the anions are in a *cis* arrangement while the wider N2-K2-N2″ angle of 127.05(6)° is due to the *trans*-indenyl orientation relative to K2.

A determining factor for the difference in the structures of $[Li(NH_3)_4][Ind]$ (**1**) and $[Na(NH_3)_4][Ind]$ (**2**) is the relative stability of the tetrahedral and square-planar-coordinated cation. We accomplished electronic structure calculations to obtain further details on the energetics of the two systems. They were performed with density-fitted local second-order Møller–Plesset perturbation theory (DF-LMP2).[12] For both Li^+ and Na^+, the T_d-symmetrical conformation is most stable. The square-planar complexes (D_{2d}-symmetrical) are somewhat higher in energy. As shown in Figure 4, the difference in the $Li(NH_3)_4^+$ case (ΔE_{conf}) is 40.7 kJ mol^{-1}, which is significantly larger than the difference in $Na(NH_3)_4^+$ (15.2 kJ mol^{-1}). This can be understood by examining the X^+-NH_3 (X = Li,Na) interaction potentials shown in Figure 5. The arrows indicate the X–N distance in each of the complexes. Considering the Li^+–NH_3 interaction curve, displacement of NH_3 from 2.119 (T_d) to 2.218 Å (D_{2d}) carries an energy penalty of 6.7 kJ mol^{-1}. In the case of Na^+, this corresponds to only 0.7 kJ mol^{-1}. From the metal–ammonia interaction alone the change in geometry leads to a 24.0 kJ mol^{-1} difference between the two metals. The energy profile is much flatter in the case of Na^+. Small changes in geometry can therefore have a larger penalty for $Li(NH_3)_4^+$ cations.

We also carried out calculations on a model system for the Ind^- sheets, embedding a single complexed cation between two anions. The geometries of the coordinated alkali metal

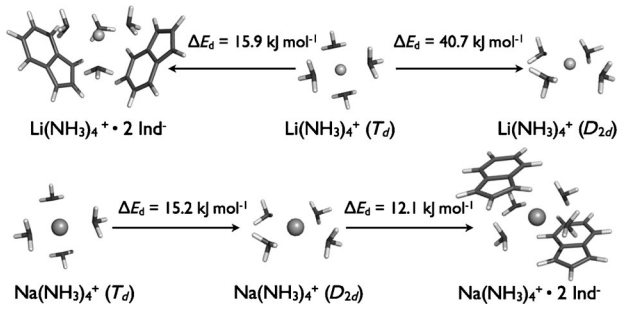

Figure 4. Deformation energies (E_d) of the complexes $Li(NH_3)_4^+$ and $Na(NH_3)_4^+$ in different conformations/constraints (T_d, D_{2d} conformations and in between Ind^- sheets).

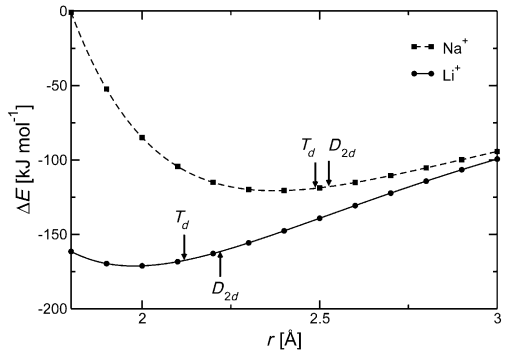

Figure 5. Potential energy curves for the X^+–NH_3 systems (X = Li, Na), with respect to the X–N distance. The *r*(X–N) values for the free complexes shown in Figure 4 are marked with arrows.

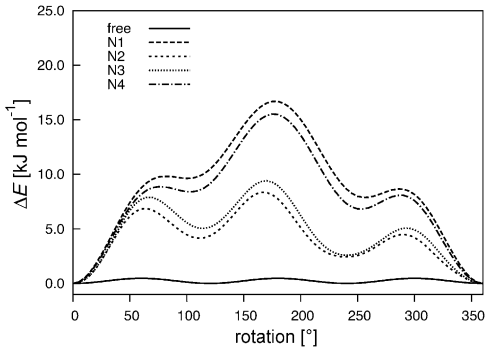

Figure 6. Potential energy curves for rotation about the Na–NH_3 bond.

cations were relaxed, with the planes constrained to the crystallographic positions. The ammine structures are only slightly distorted relative to the isolated complexes. The deformation energies are also relatively small, namely 15.9 and 12.1 kJ mol^{-1} for Li (T_d) and Na (D_{2d}), respectively (Figure 4). This can also be observed in the crystal structure. The N-Na1-N angles deviate between 0.75 and 4.52° from the ideal square-planar geometry. The sodium atom is dislocated about 0.091(2) Å from the best plane of the four nitrogen atoms, resulting in a slight pyramidality.

The relatively small difference in energy of the tetrahedral $Na(NH_3)_4^+$ compared to the square-planar form invokes the question of the actual driving force to give the solid-state structure. In fact, it can be attributed to H···π-interactions[13] of the indenyl π-system with hydrogen atoms of the ammonia molecules. This type of interaction plays a crucial role in IndLi·D complexes (D = TMEDA, THF, PMDETA, sparteine), leading to geometries that were not anticipated sterically.[14] In **1**, one hydrogen atom of each N2 and N3 is pointing towards the six-membered ring of the indenyl anions with a distance of 2.52(2) Å ($H2_C$) and 2.47(2) Å ($H3_A$), respectively. $H4_A$ of N4 is located above C2, and slightly shifted aside, with a distance of 2.54(2) Å to the ring plane. In contrast to the other ammonia molecules, the hydrogen atoms of N1 show no significant interaction to any indenyl anion within the crystal structure, which is mirrored in the rotational disorder of the hydrogen atoms.

We now look in further detail to our theoretical results on the model system of **1**. In the optimized geometries, the ammine slides even more between the Ind^- sheets compared to the crystal structure, underlining the preference to form H···π interactions, which are disturbed for N1 by crystal effects in the crystal structure. However, in both experimental and theoretical structures, the preferred orientation of the hydrogen atoms towards the Ind^- planes is visible. The same model system as discussed previously was also used to study the rotational barriers of the ammonia molecules. A rigid scan along the rotation dihedral angle of Na–N was performed for every ammonia molecule in the complex. As can be seen from Figure 6, the free state without any interaction with Ind^- only exhibits a marginal rational barrier of 0.5 kJ mol^{-1}. In contrast to this, the ammonia in the full model system need to overcome significantly higher rotational barriers of 16 kJ mol^{-1} for N1 and N4 interacting with the five-membered ring to 7 kJ mol^{-1} for N2 and N3, interacting with the six-membered ring, respectively. It should be noted that owing to the rigid scan, causing a tumbling motion of the ammonia, the rotational profiles do not exhibit a symmetric behavior after rotation by 120° as would be expected for a relaxed scan.

H···π-interaction also causes a distortion of the $Li(NH_3)_4^+$ tetrahedron in **2**, as well as the acute and widened N-K-N angles in $[(H_3N)_2K(Ind)]_\infty$ (**3**). In **2**, one hydrogen atom of each N1 and N2 points towards one indenyl anion and one hydrogen atom of N1 and another from N4 points to a second. The H···Ind distances are slightly longer for hydrogen atoms pointing to six-membered rings ($H2_A$ 2.72(2) Å, $H1_C$ 2.55(2) Å) compared to interactions with the more highly charged five-membered rings ($H1_A$ 2.47(2) Å, $H4_A$ 2.49(2) Å). N3 in **2** shows no interaction with any Ind^- within the crystal structure, like N1 in **1**. The $Li(NH_3)_4^+$ cation is coordinated at adjacent sides of the tetrahedron, giving rise to the observed zigzag packing within the crystal. The indenyl anions do not adjust perfectly to the shape of the cation, but rather pulling the ammonia molecules away from the ideal position, widening the N2-Li1-N4 angle to 121.95° and emphasizing the strength of the H···π interactions.

The strength of the operating H···π-interaction is even more obvious in **3**, when no solvent separation takes place.

Within this structure as well, NH_3 hydrogen atoms are placed above and below the C_6 perimeter, while the C_5 perimeter is exclusively reserved for the metal atoms. The H···Ind distances of 2.59(2) Å ($H1_C$) and 2.74(2) Å ($H2_B$) are even smaller than the K···Ind distances of 2.8811(6) Å (K1) and 2.8712(6) Å (K2). This effect reduces the N1-K1-N1′ angle to 88.87°(8) and widens the N2-K2-N2″ angle to 127.05°(6).

In conclusion, we have shown that the unprecedented layered structure of $[Na(NH_3)_4][Ind]$, consisting of alternating square-planar cation layers and self-assembled indenyl anion layers, is caused by two facts: the energy difference between T_d-symmetric $Na(NH_3)_4^+$ to D_{2d} square-planar is about 25 kJ mol^{-1} lower than in the $Li(NH_3)_4^+$ case. Furthermore, the small energy penalty can easily be compensated by additional NH···π interactions.

Experimental Section

Single-crystal structural analysis: Single crystals were mounted in inert oil under protective atmosphere by applying the X-Temp2 device.[15] The X-ray data sets of **1–3** were collected at 100(2) K on a Bruker Smart Apex II Quazar diffractometer equipped with an INCOATEC microfocus source[16] with mirror-monochromated Mo-Kα radiation ($\lambda = 0.71073$ Å). The structures were solved by direct methods with SHELXS and refined by full-matrix least-squares on F^2 for all data with SHELXL.[17] Non-hydrogen atoms were refined with anisotropic displacement parameters. Nitrogen-bound hydrogen atoms were located in the difference Fourier map and refined isotropically using distance similarity restraints for all N–H and H···H-1,2-distances. All other hydrogen atoms were placed in calculated positions and refined using a riding model.

1: $C_9H_{19}N_4Na$, $M = 206.27$ g mol^{-1}, monoclinic, space group $P2_1$, $a = 6.865(2)$, $b = 14.391(3)$, $c = 6.966(3)$ Å, $\beta = 117.70°(2)$, $V = 609.3(3)$ Å^3, $Z = 2$, $\mu(MoK_\alpha) = 0.102$ mm^{-1}, 30085 reflections measured, 1858 unique reflections ($R_{int} = 3.53\,\%$), $\Theta_{max} = 30.05°$, 177 parameters refined, 211 restraints used, R_1(all data) = 3.11 %, wR_2-[$I > 2\sigma(I)$] = 8.20 %, GooF = 1.072, largest diff. peak and hole 0.313 and −0.158 e Å^{-3}. The absolute structure could not be determined successfully.

2: $C_9H_{19}N_4Li$, $M = 190.22$ g mol^{-1}, orthorhombic, space group $P2_12_12_1$, $a = 8.492(4)$, $b = 10.262(3)$, $c = 13.445(6)$ Å, $V = 1171.7(8)$ Å^3, $Z = 4$, $\mu(MoK_\alpha) = 0.067$ mm^{-1}, 20621 reflections measured, 4839 unique reflections ($R_{int} = 2.38\,\%$), 167 parameters refined, 132 restraints used, R_1(all data) = 4.02 %, $wR_2[I > 2\sigma(I)] = 8.82\,\%$, GooF = 1.082, largest diff. peak and hole 0.327 and −0.153 e Å^{-3}. The absolute structure could not be determined successfully.

3: $C_9H_{13}N_2K$, $M = 188.31$ g mol^{-1}, orthorhombic, space group $Fddd$, $a = 18.318(2)$, $b = 19.172(2)$, $c = 23.841(3)$ Å, $V = 8372.8(2)$ Å^3, $Z = 32$, $\mu(MoK_\alpha) = 0.459$ mm^{-1}, 38900 reflections measured, 3201 unique reflections ($R_{int} = 4.51\,\%$), 128 parameters refined, 30 restraints used, R_1(all data) = 4.13 %, $wR_2[I > 2\sigma(I)] = 7.41\,\%$, GooF = 1.056, largest diff. peak and hole 0.416 and −0.205 e Å^{-3}.

CCDC 891478 (**1**), 891477 (**2**), and 898399 (**3**) contain the supplementary crystallographic data for this paper. These data can be obtained free of charge from The Cambridge Crystallographic Data Centre via www.ccdc.cam.ac.uk/data_request/cif.

Computational details: All calculations were carried out at the DF-LMP2 level[12] with the Molpro2010.1 program package.[18] The orbital basis set used was cc-pVTZ for all atoms, except Li and Na (cc-pCVTZ). The density-fitting basis sets were cc-pVTZ/JKFIT and cc-pVTZ/MP2FIT (def2-TZVPP/JKFIT and cc-pwCVTZ/MP2FIT for the alkali atoms).[19] All electrons were included in the correlation calculations except for the 1s electrons of Na. No symmetry constrains were applied in the geometry optimizations. The planar complexes of $Li(NH_3)_4^+$ and $Na(NH_3)_4^+$ were optimized keeping the alkali atoms in a plane with the N atoms (non-minima at the potential energy surface). In the local correlation treatment, the orbitals were localized according to the Pipek–Mezey criteria and the domains selected with a NPA criterion $T_{NPA} = 0.03$.[20] The Na^+–NH_3 potential curve was generated from a relaxed distance scan (only the Na–N interatomic distance was kept frozen). The $X(NH_3)_4^+ \cdot 2\,Ind^-$ (X = Li,Na) models were built by optimizing the Ind^- anion and placing two units in the crystallographic positions by a root-mean-square fit of the C atom positions. The rotation profiles in Figure 6 were computed by simultaneously varying the H-N-Na-H′ angle of all the hydrogen atoms (H) in a single ammonia molecule relative to another hydrogen atom (H′). The orbital domains were kept constant in all of the energy profiles.[21]

Received: August 31, 2012
Published online: November 21, 2012

Keywords: ammonia · carbanions · hydrogen bonds · lithium · sodium

[1] M. Winter, J. O. Besenhard, M. E. Spahr, P. Novák, *Adv. Mater.* **1998**, *10*, 725–763.
[2] a) D. Savoia, C. Trombini, A. Umani-Ronchi, *Pure Appl. Chem.* **1985**, *57*, 1887–1896; b) S. Khan, R. Michel, J. M. Dieterich, R. A. Mata, H. W. Roesky, J.-P. Demers, A. Lange, D. Stalke, *J. Am. Chem. Soc.* **2011**, *133*, 17889–17894.
[3] N. Emery, C. Hérold, J.-F. Marêché, P. Lagrange, *Sci. Technol. Adv. Mater.* **2008**, *9*, 044102.
[4] a) M. A. Petrukhina, L. T. Scott, *Fragments of Fullerenes and Carbon Nanotubes: Designed Synthesis, Unusual Reactions, and Coordination Chemistry*, Wiley, Hoboken, NJ, **2012**; b) A. V. Zabula, S. N. Spisak, A. S. Filatov, M. A. Petrukhina, *Organometallics* **2012**, *31*, 5541–5545; c) A. V. Zabula, A. S. Filatov, S. N. Spisak, A. Y. Rogachev, M. A. Petrukhina, *Science* **2011**, *333*, 1008–1011; d) R. Haag, R. Fleischer, D. Stalke, A. de Meijere, *Angew. Chem.* **1995**, *107*, 1642–1644; *Angew. Chem. Int. Ed. Engl.* **1995**, *34*, 1492–1495; e) A. Ayalon, A. Sygula, P.-C. Cheng, M. Rabinovitz, P. W. Rabideau, L. T. Scott, *Science* **1994**, *265*, 1065–1067.
[5] P. He, H. Yu, D. Li, H. Zhou, *J. Mater. Chem.* **2012**, *22*, 3680–3695.
[6] a) T. P. Ying, X. L. Chen, G. Wang, S. F. Jin, T. T. Zhou, X. F. Lai, H. Zhang, W. Y. Wang, *Sci. Rep.* **2012**, *2*, 426, DOI: 10.1038/srep00426; b) E.-W. Scheidt, V. R. Hathwar, D. Schmitz, A. Dunbar, W. Scherer, V. Tsurkan, J. Deisenhofer, A. Loidl, *Cond. Matter arXiv.org, e-Print Arch.* **2012**, arXiv:1205.5731v1201.
[7] a) P. Jutzi, N. Burford, *Chem. Rev.* **1999**, *99*, 969–990; b) N. J. Long, *Metallocenes*, Blackwell Science Malden, MA, **1998**; c) S. Harder, *Coord. Chem. Rev.* **1998**, *176*, 17–66; d) D. Stalke, *Angew. Chem.* **1994**, *106*, 2256–2259; *Angew. Chem. Int. Ed. Engl.* **1994**, *33*, 2168–2171; e) A. Raith, P. Altmann, M. Cokoja, W. A. Herrmann, F. E. Kühn, *Coord. Chem. Rev.* **2010**, *254*, 608–634; f) R. Theys, M. E. Dudley, M. M. Hossain, *Coord. Chem. Rev.* **2009**, *253*, 180–234; g) M. Sharma, M. S. Eisen, *Struct. Bonding (Berlin)* **2008**, *127*, 1–85; h) M. Tamm, *Chem. Commun.* **2008**, 3089–3100; i) "Lead Structures in Lithium Organic Chemistry": T. Stey, D. Stalke in *The Chemistry of Organolithium Compounds* (Eds.: Z. Rappoport, I. Marek), Wiley, Chichester, **2004**, pp. 47–120.
[8] R. Michel, R. Herbst-Irmer, D. Stalke, *Organometallics* **2010**, *29*, 6169–6171.
[9] *CRC Handbook of Chemistry and Physics*, *87th ed.*, Taylor & Francis, Boca Raton, FL, **2006**.
[10] F. H. Allen, *Acta Crystallogr. Sect. B* **2002**, *58*, 380–388.
[11] V. Jordan, U. Behrens, F. Olbrich, E. Weiss, *J. Organomet. Chem.* **1996**, *517*, 81–88.

[12] H.-J. Werner, F. R. Manby, P. J. Knowles, *J. Chem. Phys.* **2003**, *118*, 8149 – 8160.
[13] a) T. Steiner, *Angew. Chem.* **2002**, *114*, 50 – 80; *Angew. Chem. Int. Ed.* **2002**, *41*, 48 – 76; b) "The Weak Hydrogen Bond": G. R. Desiraju, T. Steiner in *IUCr Monographs on Crystallography 9*, Oxford University Press, Oxford, **1999**.
[14] R. Michel, R. Herbst-Irmer, D. Stalke, *Organometallics* **2011**, *30*, 4379 – 4386.
[15] a) D. Stalke, *Chem. Soc. Rev.* **1998**, *27*, 171 – 178; b) T. Kottke, D. Stalke, *J. Appl. Crystallogr.* **1993**, *26*, 615 – 619.
[16] T. Schulz, K. Meindl, D. Leusser, D. Stern, J. Graf, C. Michaelsen, M. Ruf, G. M. Sheldrick, D. Stalke, *J. Appl. Crystallogr.* **2009**, *42*, 885 – 891.
[17] a) G. M. Sheldrick, *Acta Crystallogr. Sect. A* **2008**, *64*, 112 – 122; b) P. Müller, R. Herbst-Irmer, A. L. Spek, T. R. Schneider, M. R. Sawaya, *Crystal Structure Refinement—A Crystallographer's Guide to SHELXL*, Oxford University Press, Oxford (England), **2006**.
[18] H.-J. Werner, P. J. Knowles, G. Knizia, F. R. Manby, M. Schütz, MOLPRO, version 2010.1, a package of ab initio programs 2010, http://www.molpro.net.
[19] a) T. H. Dunning, *J. Chem. Phys.* **1989**, *90*, 1007 – 1023; b) B. P. Prascher, D. E. Woon, K. A. Peterson, T. H. Dunning, A. K. Wilson, *Theor. Chim. Acta* **2011**, *128*, 69 – 82; c) F. Weigend, *Phys. Chem. Chem. Phys.* **2002**, *4*, 4285 – 4291; d) F. Weigend, *J. Comput. Chem.* **2008**, *29*, 167 – 175; e) D. Rappoport, F. Furche, *J. Chem. Phys.* **2010**, *133*, 134105; f) F. Weigend, M. Häser, H. Patzelt, R. Ahlrichs, *Chem. Phys. Lett.* **1998**, *294*, 143 – 152; g) C. Hättig, *Phys. Chem. Chem. Phys.* **2005**, *7*, 59 – 66.
[20] R. A. Mata, H.-J. Werner, *Mol. Phys.* **2007**, *105*, 2753 – 2761.
[21] R. A. Mata, H.-J. Werner, *J. Chem. Phys.* **2006**, *125*, 184110.

